PERGAMON

International Journal of Solids and Structures 37 (2000) 6383–6395

INTERNATIONAL JOURNAL OF SOLIDS and STRUCTURES

www.elsevier.com/locate/ijsolstr

A one-dimensional model for designing functionally graded materials to manage stress waves

Hugh A. Bruck

Department of Mechanical Engineering, University of Maryland, College Park, MD 20742, USA

Received 14 April 1998; in revised form 26 August 1999

Abstract

The development of Functionally Graded Materials (FGMs) for energy-absorbing applications requires understanding of stress wave propagation in these structures in order to optimize their resistance to failure. A simple, one-dimensional model is proposed to develop insight into stress wave management issues. This model is initially applied to FGMs with discrete layering, then extended to continuously graded architectures. From this model, it is determined that the peak stress of waves reflected from the FGM interface is slightly greater than for materials with sharp interfaces. The benefit of the FGM over the sharp interface is to introduce a time delay to the reflected wave propagation when stresses approach peak levels. This time delay is highly dependent on the composition gradient and the differences in base material properties, consequently the optimal choice of FGM architecture will depend significantly on the critical design conditions for specific applications. Time-history profiles of reflected stress waves are presented for two specific cases of interest in armor applications: (1) porous FGMs, and (2) Alumina–Aluminum FGMs.

Keywords: Functionally graded materials; Armor; Stress wave propagation

1. Introduction

There is a great deal of interest in developing Functionally Graded Materials (FGMs) for joining dissimilar materials in energy absorbing applications, such as armor plating. The advantage of using FGMs is their superior resistance to interfacial failure. In addition, it has been postulated that the graded interface will attenuate stress wave propagation. The effect of graded interfaces on stress wave propagation has not yet been investigated.

FGMs have been manufactured using a variety of techniques, such as thermal spray processing, powder processing, and infiltration casting (see e.g. Mortenson and Suresh, 1994). Previous design studies on FGMs have focused on examining the effects of gradient architecture on thermal residual stresses and fracture (see e.g. Williamson et al., 1993; Williamson and Rabin, 1996; Finot and Suresh,

0020-7683/00/$ - see front matter
PII: S0020-7683(99)00236-X

1996). For example, Williamson and Rabin (1996) have concluded that designing the interface of a cylindrical FGM with as few as four discrete layers with a composition gradient of $(x/d)^3$, where x is the distance from the first base material and d is the thickness of the interface, can minimize thermal residual stresses. While this architecture may be suitable for addressing fabrication issues, it is still necessary to determine architectural features that are desirable to manage stress wave propagation. Kuwahara et al. (1992) have proposed an NDE technique using Howard's inverse scattering method to characterize the acoustic impedance profile of FGMs. However, this technique only analyzes the effects of the graded interface on the frequency response of the stress waves, not their propagation behavior.

In this paper, a simple one-dimensional (1D) model is presented for analyzing stress wave propagation in FGMs. Gradient architectures are examined to determine optimal characteristics for the design of FGMs to manage stress waves. Design examples are also presented for two cases of interest in armor applications: (1) a porous FGM, and (2) an Alumina–Aluminum FGM.

2. Theoretical model

In designing FGMs for energy absorbing applications, it is necessary to understand the types of loading to which the system will be subjected. For impact events, many different types of stress waves (e.g., Rayleigh, dilitational) are initially generated and propagate in a 3D manner (see e.g. Wilkins et al., 1970). Of these waves, the compressive dilitational waves usually contain most of the energy generated by the impact and are fairly focused ahead of the impact zone. During propagation through an energy absorbing system containing dissimilar materials, where the impacted material is typically harder than the backing material, the compressive wave will be reflected as a tensile wave at an interface. In many applications, these tensile waves start compromising the structural integrity of the system components, leading to localized system failure. Therefore, in designing interfaces for these systems it is desirable to attenuate the reflection of stress waves to delay the failure of individual components, thereby de-localizing system failure. In order to analyze the impact behavior of FGMs, stress waves will be modeled as linearly elastic, longitudinal waves propagating in one dimension.

The next issue to be addressed is the modeling of the gradient architecture formed from base materials 1 and 2, designated by $V = 0$ and $V = 1$, respectively in Fig. 1. Previous studies have typically treated the graded interlayer as a system of discrete layers that can be infinitely refined to a

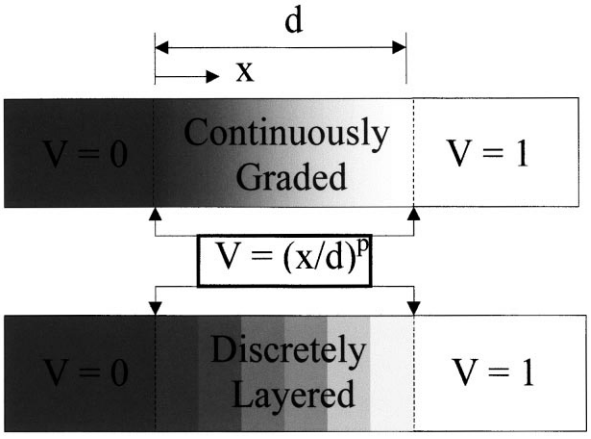

Fig. 1. Gradient architecture of FGMs.

continuous gradient (Markworth et al., 1995). These layers are usually identical in size, but follow a power-law variation in composition as follows,

$$V = \left(\frac{x}{d}\right)^n \tag{1}$$

where V is the volume fraction of base material 2 and n is an exponent that can be arbitrarily varied.

3. One-dimensional stress wave propagation in discretely layered FGMs

Using the aforementioned assumptions, stress wave propagation in discretely layered FGMs can now be visualized in Fig. 2. If the graded interface consists of m discretely graded layers between base materials 1 and 2, then the propagating stress wave will encounter $m+1$ sharp interfaces. At each sharp interface, the stress wave will be partially reflected and transmitted. For 1D wave propagation, the amount of reflection and transmission from a sharp interface can be determined as follows (see e.g. Meyers (1994)):

$$f = \frac{2f_i}{(1+\alpha)} \tag{2a}$$

$$f_r = f_i \frac{(1-\alpha)}{(1+\alpha)} \tag{2b}$$

where f_i is the amount of stress in the incident wave, f_t is the amount of stress in the transmitted wave, f_r is the amount of stress in the reflected wave, and α is the ratio of the acoustic impedance of base material 1 to the acoustic impedance of base material 2. The thickness of each layer is $\frac{d}{m}$, and the total time, t, it takes for the incident wave to travel through a layer and then get reflected back is:

$$t = \frac{2d}{cm} \tag{3}$$

where c is the longitudinal wave speed of the layer.

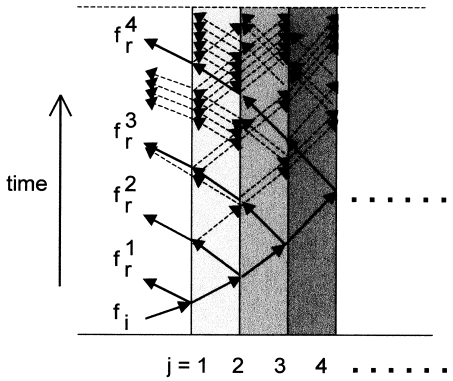

Fig. 2. One-dimensional stress wave propagation through discretely layered FGM (note the waves reflected from multiple interfaces, designated by dashed arrows).

A time-history profile of the stress wave reflected into base material 1 by the graded interface can now be constructed by summing the waves reflected from each discrete layer and the time it takes for that wave to be generated and reach base material 1. Assuming that the period of the stress wavelength, λ, is much longer than the thickness of the graded interface (i.e., $\lambda \gg$ d), the normalized magnitude of the reflected wave in base material 1 will be,

$$\frac{f_{\mathrm{r}}^{1}}{f_{\mathrm{i}}} = \frac{1-\alpha_0}{1+\alpha_0} + \sum_{j=1}^{m}\left[\frac{(1-\alpha_j)}{(1+\alpha_j)}\prod_{k=1}^{j}\frac{4\alpha_{k-1}}{(1+\alpha_{k-1})^2}\right] + \text{HOTs} \tag{4}$$

where f_{r}^{1} is the amount of stress in the wave reflected into base material 1, α_j is the ratio of acoustic impedance of layer $j+1$ to j, and HOTs are higher order terms comprised of three or more reflections and one or more transmissions. Note that layer 0 and layer $m+1$ are base materials 1 and 2 respectively, and each intermediate layer is a composite of the two base materials whose exact composition is determined using Eq. (1). The normalized time it takes for the wave reflected from the jth layer to reach base material 1, $\bar{t}$, is given by,

$$\bar{t} = \frac{t^1}{(d/c_0)} = \frac{2}{m}\sum_{k=1}^{f}\frac{c_0}{c_k} \tag{5}$$

where t^1 is the time it takes to reach base material 1, c_0 is the wave speed in base material 1, and c_k is the wave speed in layer k.

The HOTs in Eq. (4) have the following form,

$$(-1)^p\left[\frac{(1-\alpha)}{(1+\alpha)}\right]^{2p+1}\left[\frac{4\alpha}{(1+\alpha)^2}\right]^{q} = (-1)^p R T \quad p\geq 1,\ q\geq 1 \tag{6}$$

where $-1 < R < 1$ represents the product resulting from each reflection that the propagating stress wave experiences at a sharp interface between layers in the graded interface, as indicated in the left-hand side of Eq. (6), and $0 < T < 1$ represents the product resulting from each transmission. Since $T\to 0$ as $R\to 1$, -1 and $R\to 0$ as $T\to 1$, the contribution of each HOT gets progressively smaller as p and q increase. Consequently, the largest individual contribution comes when $p = q = 1$.

Considering the case where the graded interlayer is comprised of a single layer. Let $\alpha > 1$ on the first interface of the interlayer and the second interface has an $\alpha \gg 1$. The magnitude of the first HOT term can then be compared with the magnitude of the first two terms in Eq. (4). From this comparison, it can be seen that the contribution of the first HOT is greatest when $\alpha = 4$, where the magnitude of the HOT will be 31% of the first two terms that result from waves reflected from the front and back interfaces of the layer. For $p > 1$, the corresponding HOT will be $(-0.6)^{p-1}$ of the first HOT, which will help to reduce the contribution of all HOTs to 19%. Similar contributions are also obtained if the first interface has $\alpha < 1$ and the second interface has $\alpha \ll 1$. While it appears that the contributions from HOT can not always be neglected, it is simpler to extend the analysis to a continuously graded interface by neglecting all of the HOTs.

4. Stress wave propagation in continuously graded FGMs

In order to analyze the effects of the gradient architecture on stress wave propagation in continuous FGMs, assume that the normalized physical properties of each layer can be described using a linear rule-of-mixtures (ROM) formula as follows:

$$\frac{p_j}{p_0} = 1 + (\bar{p} - 1)V_j \tag{7}$$

where p_0 is the property of base material 1, $\bar{p}$ is the ratio of the property for base material 2 to the property for base material 1, and p_j is the property of the jth layer. Also, assume that the acoustic impedance obeys the linear ROM formulation.

By infinitely refining the discrete analysis used to develop Eqs. (4) and (5), an analytic expression can be derived for the behavior for a continuously graded interface as follows for an arbitrary n, as follows:

$$\frac{f_r}{f_i} = \frac{1}{2}\int_0^{x/d} (\bar{\kappa} - 1)n\tau^{n-1}(1 + (\bar{\kappa} - 1)\tau^n)^{-1}\,\mathrm{d}\tau = \frac{1}{2}\ln\left(1 + (\bar{\kappa} - 1)\left(\frac{x}{d}\right)^n\right) \tag{8a}$$

$$\frac{tc_0}{d} = 2\int_0^{\frac{x}{d}} (1 + (\bar{\kappa} - 1)\tau^n)^{-1}\,\mathrm{d}\tau \tag{8b}$$

where $\frac{x}{d} \leq 1$, and $\bar{\kappa}$ is the acoustic impedance of base material 2 normalized by the acoustic impedance of base material 1. From these equations, it can be seen that the peak reflected stress will be independent of n and is equal to $\ln(\bar{\kappa})$.

As $n \to 0$ and $n \to \infty$, the gradient architecture will approach the case of a sharp interface. In both of these cases, the peak magnitude predicted by Eq. (8a) should be identical to the magnitude of a wave reflected from sharp interface. However, the peak magnitude of the stress wave, which occurs at $x = d$, actually exceeds that of a sharp interface by a factor of $\frac{(1+\bar{\kappa})}{2(1-\bar{\kappa})}\ln(\bar{\kappa})$. This discrepancy is a direct result of neglecting the contribution of HOTs in the analysis. Differences in the magnitude of the peak stress will be negligible as $\bar{\kappa} \to 1$, however they will approach infinity as $\bar{\kappa} \to 0$ and $\bar{\kappa} \to \infty$.

While Eq. (8a) appears to be inadequate for predicting the magnitude of stress waves reflected from sharp interfaces as $\bar{\kappa} \to 0$ and $\bar{\kappa} \to \infty$, it can be seen that for cases where $(\bar{\kappa} - 1)(\frac{x}{d})^n \ll 1$, Eq. (8a) can be approximated as follows,

$$\frac{f_r}{f_t} \sim \frac{(\bar{\kappa} - 1)\left(\frac{x}{d}\right)^n}{2} \tag{9}$$

The right-hand side of Eq. (9) is also approximately equal to

$$\frac{\left[1 - \frac{\kappa(x)}{\kappa(0)}\right]}{\left[1 + \frac{\kappa(x)}{\kappa(0)}\right]} \quad \text{for } (\bar{\kappa} - 1)\left(\frac{x}{d}\right)^n \ll 1$$

which also produces the correct result for a sharp interface at $x = d$. It can now be determined heuristically argued that the following equation will more accurately predict the magnitude of the reflected stress waves,

$$\frac{f_r}{f_i} \sim \frac{\left[1 - \frac{\kappa(x)}{\kappa(0)}\right]}{\left[1 + \frac{\kappa(x)}{\kappa(0)}\right]} \tag{10}$$

Eq. (10) is an analytic expression that may better capture the effects of HOTs neglected in the

development of Eq. (8a). This can be verified by performing a numerical simulation of the stress wave propagation in FGMs.

5. Numerical simulation of stress wave propagation in discretely layered FGMs

A numerical code was developed for analyzing the propagation of stress waves in discretely layered FGMs. This code tracks the propagation of reflected stress waves in the FGM interlayer. Because the number of stress waves reflected in the interlayer increases very rapidly with time, an Eulerian description of the stress wave propagation was used in the numerical analysis. This description involved subdividing each layer of the FGM into 'nodal locations' where the direction and magnitude of each wave was calculated. Discrete time increments were also used to calculate the propagation of the stress waves. Since the calculated positions may not always correspond to 'nodal locations', there will be some error introduced into the analysis that can be minimized by using small time increments and finer resolution of the 'nodal locations'.

As was previously mentioned, the effects of HOTs appear to be more significant as $\bar{\kappa}\rightarrow 0$ and $\bar{\kappa}\rightarrow\infty$. Therefore, a numerical simulation will be performed using $\bar{\kappa}=0.01$, which from Eq. (8a) corresponds to a reflected stress wave with a peak magnitude that is 2.4 times greater than the reflection from a sharp interface. The time-history for the reflected stress waves predicted from the numerical simulation for various discretely layered architectures can be seen in Fig. 3 for $n=1$. From this figure, it appears that as the architecture becomes continuously graded, Eq. (10) is far more accurate in predicting the time-history of the reflected stress wave than Eq. (8a). In fact, the steady-state magnitude of the reflected stress wave is independent of the layering and is identical to the response for a sharp interface.

The effects of the composition gradient on the time-history for the reflected stress wave can be seen in

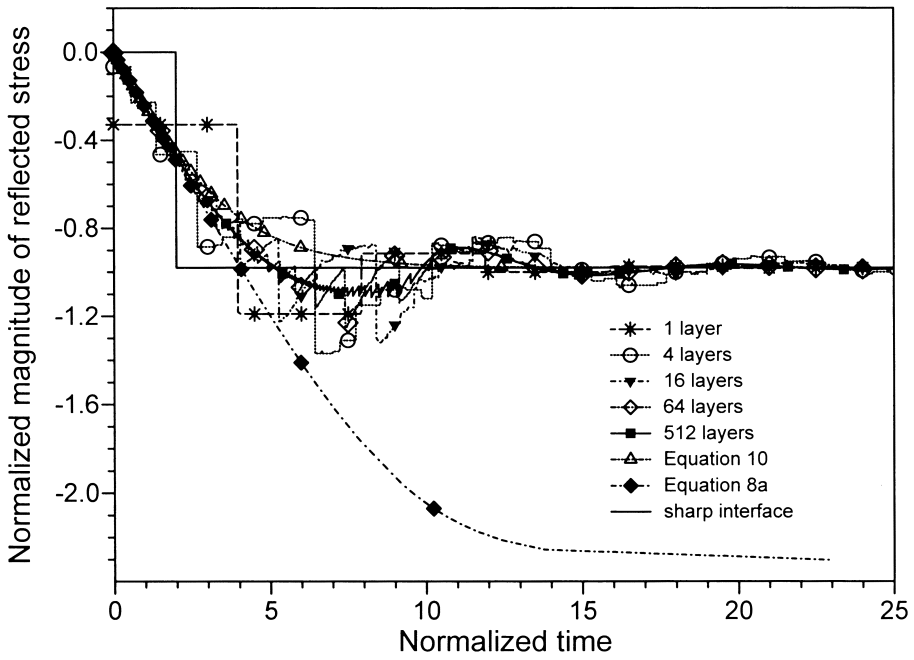

Fig. 3. Numerical simulation of discrete layering effects on reflected wave propagation in a FGM with $\bar{\kappa}=0.01$ and $n=1$.

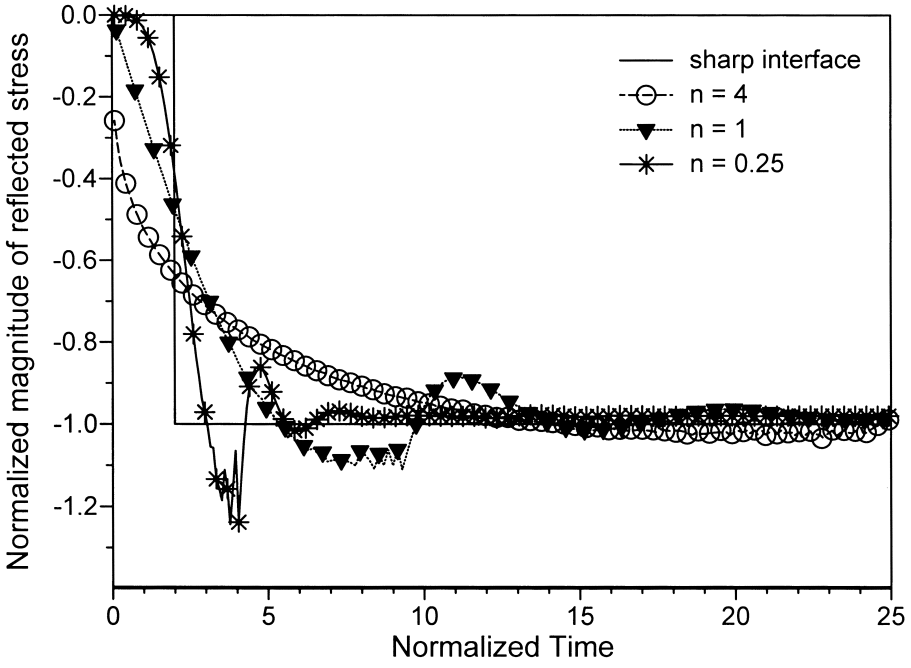

Fig. 4. Effects of composition gradient on time-history of reflected stress wave.

Fig. 4. This figure indicates that the time when stresses approaching peak levels occur in the FGM is delayed over the sharp interface. Furthermore, the time to these stress levels increases substantially as n approaches 0. This time delay can result in a greater dynamic energy absorbing capability for the FGM architecture over a sharp interface architecture by delaying the time it takes to initiate damage. Thus, even though the peak stress is unaffected by the gradient architecture, there can be a time delay benefit

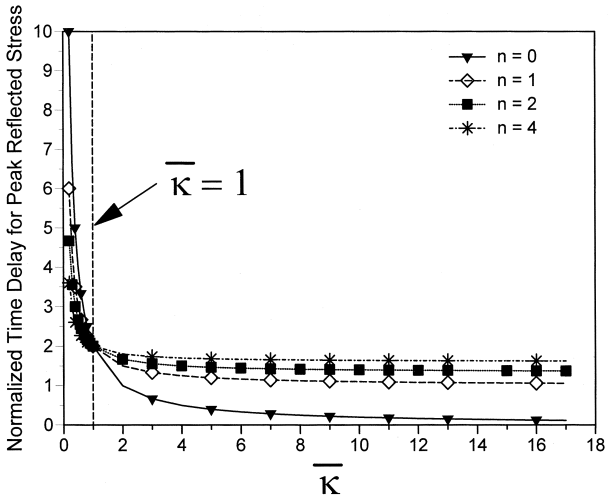

Fig. 5. effects of gradient architecture on the normalized time delay for the peak reflected stress.

to using an FGM. Using Eq. (10), the effect of gradient architecture on the time delay to the peak reflected stress is summarized in Fig. 5. This time delay benefit only exists for $\bar{\kappa} < 1$, which is not surprising since for $\bar{\kappa} > 1$ the reflected waves will be traveling much faster through the interlayer than through base material 1. Furthermore, the time delay appears to be optimal when $\bar{\kappa} \to 0$, which corresponds to a porous FGM. Since this case appears to be of benefit in optimizing the design of FGMs for stress wave management, it will be considered in more detail in Section 6.

While Eq. (10) appears to capture the wave propagation trends predicted for discretely layered FGMs, even for a single layered architecture, the response of a continuously graded FGM still oscillates around the response predicted from Eq. (10). This 'overshoot' behavior occurs near the peak reflected stress, and is similar to the response that would be expected from an underdamped, fourth-order system feedback control system with a step input equivalent to the wave reflected from a sharp interface as follows (see e.g. Dorf, 1986):

$$\frac{f_r}{f_i} = \frac{[1-\bar{\kappa}]}{[1+\bar{\kappa}]}\left(1 - a_1 e^{-a_2 t}\sin(a_3 t + a_4) - a_5 e^{-a_6 t}\sin(a_7 t + a_8)\right) \tag{11}$$

where a_i are arbitrary constants. Although there is no physical basis for applying Eq. (11) to the continuously graded FGM, it provides a more accurate mathematical description for the reflected stress wave than the one provided by Eq. (10). However, the unknown parameters it contains can only be determined by fitting the equation to pre-existing numerical results.

A best fit of Eq. (11) to the results of the numerical simulation for an interface with 512 layers can be seen in Fig. 6. The magnitude of the 'overshoot' appears to increase the larger n gets (Fig. 4), indicating that the remaining effects of HOTs not captured in Eq. (10) appear to increase as the changes in composition become greater farther away from the base material 1. This 'overshoot' behavior can increase the magnitude of the peak reflected stress and slightly reduce the time delay at stress levels near the peak reflected stress. However, since the benefits of the time delay to the peak reflected stress in Fig. 5 are most significant for small n, 'overshoot' effects should be minimal and Eq. (10) should be sufficient for further analyzing the time delay benefits of FGMs.

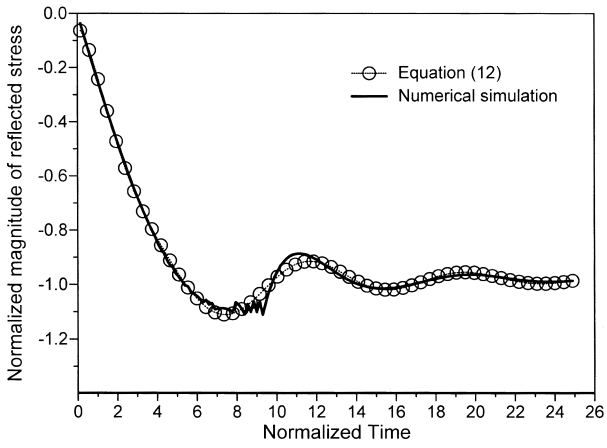

Fig. 6. Best fit of solution for an underdamped, fourth-order feedback control system to a numerical simulation of a gradient architecture with $n = 1$.

6. Special FGM cases

6.1. Case I: porous FGMs

As was previously discussed, porous FGMs may be used to optimize the management of stress waves. Porous materials are already of interest for armor applications because of their superior ballistic mass efficiency, which is a relative measure of the mass of a material that is required to resist penetration by a projectile. The variation of the time-history with n can be seen for a quasi-porous FGM with $\bar{\kappa} = 10^{-5}$ in Fig. 7. An idea of how the choice of the normalized magnitude may affect the selection of an optimal n can be seen in Fig. 8. From this figure it can be seen that the desired reflected stress must be over 50% of the steady-state level before any significant time delay benefits are obtained from the gradient architecture. Furthermore, as previously stated, time delay benefits are only realized for small gradient exponents, which significantly reduces the impact of 'overshoot' and validates the use of Eq. (10).

In reality, it is not possible to manufacture a porous material with a continuous gradient to a porosity level of 100% because connectivity issues associated with grain size will prevent a highly porous material from remaining intact. Therefore, a porous FGM will terminate in a free surface at a porosity level less than 100%. This free surface will reflect a stress wave that has a greater peak magnitude than if the free surface was not present (Fig. 9). This reflection will also decrease the time delay benefit that would have been achieved had the free surface not been present. The end result could be a peak reflected wave occurring sooner than had a sharp interface been present, which would have a deleterious effect on the energy absorbing capability of the FGM.

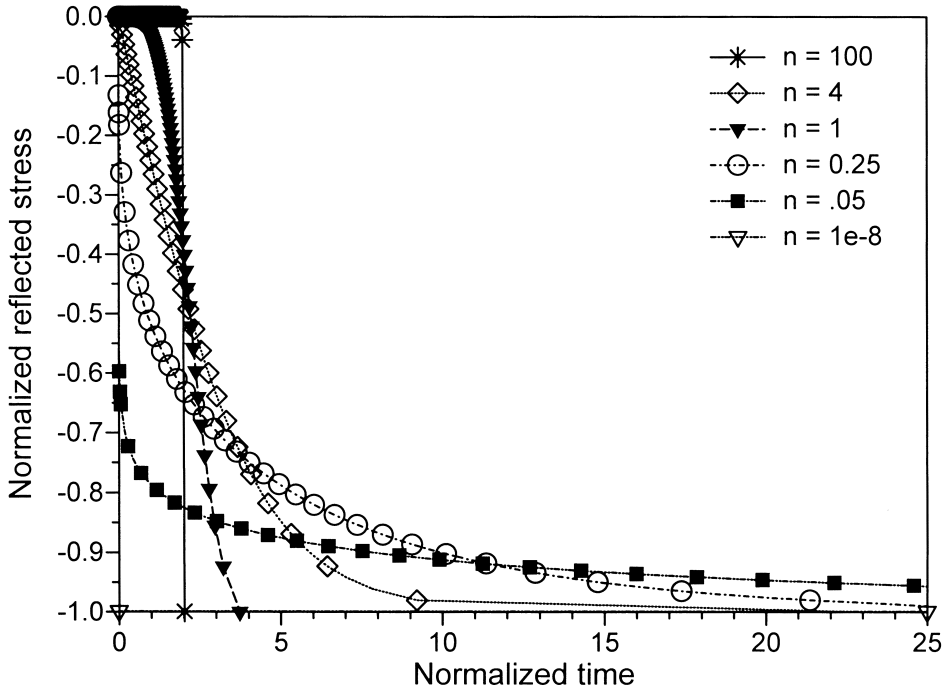

Fig. 7. Time-history profile of reflected stress wave for quasi-porous FGM with $\bar{\kappa} = 10^{-5}$.

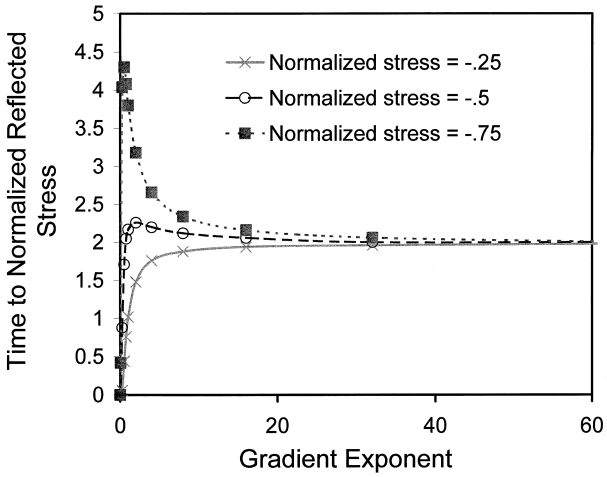

Fig. 8. Variation of time to normalized reflected stress with gradient exponent at various normalized stress levels for a quasi-porous FGM with $\bar{\kappa} = 10^{-5}$.

6.2. Case II: Alumina–Aluminum FGM

In addition to Porous FGMs, another FGM system that is of interest for armor applications is Alumina–Aluminum. The physical properties of these materials are given in Table 1. Using the ROM formulation, normalized wave speeds, $\bar{c}$, and acoustic impedances, $\bar{\kappa}$, for various volume fractions of Aluminum, V, can be determined (Fig. 10). It can be seen that these properties obey a power law form that is identical to the ones used in the previous analyses. The time-history behavior for this FGM system can now be formulated in Fig. 11, and the time delay benefits summarized in Fig. 12.

Comparing the time delay benefits of Alumina–Aluminum FGMs with quasi-porous FGMs, it is apparent that the time delay benefits are greater for the quasi-porous FGM, which possesses a greater difference in base material properties. This behavior is consistent with the efforts of the gradient architecture effects on the time to the peak reflected stress reported in Fig. 5. In fact, maximum time

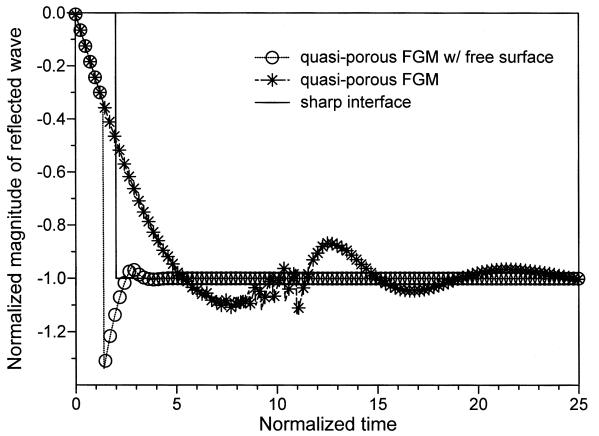

Fig. 9. Wave propagation effects for a quasi-porous FGM that is terminated in a free surface at a porosity level of 50%.

Table 1
Physical properties for Alumina and Aluminum

Property	Alumina	Aluminum
Young's modulus, E (GPa)	400	70
Density, ρ (kg/m^3)	4000	2700
Wave speed, c (km/s)	10	5

delay benefits of only 25% are expected when the stress level is within 93% of the steady-state level for the reflected stress. Thus, using gradient architectures may slightly improve the energy absorbing capability of Alumina–Aluminum structures, which is in contrast to the effect gradient architectures may have on porous FGMs.

7. Conclusions

A simple, 1D model for stress wave propagation in FGMs has been formulated. Using this model, the effects of gradient architecture on the attenuation of stress waves reflected from the interface can be analyzed for design purposes. The following conclusions can be drawn:

1. Stress wave management benefits from using FGMs can be derived using a single layered architecture.
2. The steady-state magnitude of the reflected stress wave is independent of layering and composition gradient, and is identical to the magnitude of the stress wave reflected from a sharp interface.
3. Gradient architectures have larger peak magnitudes for reflected stress waves than sharp interfaces, however the time at which stresses approaching peak levels is delayed resulting in a *time delay benefit* for $\bar{\kappa} < 1$.
4. The time delay benefits of using a FGM are greatest when the desired magnitude of the reflected stress wave approaches that for a sharp interface and the gradient exponent approaches 0.
5. Time delay benefits will be greater and occur at lower relative stress levels as the differences in base

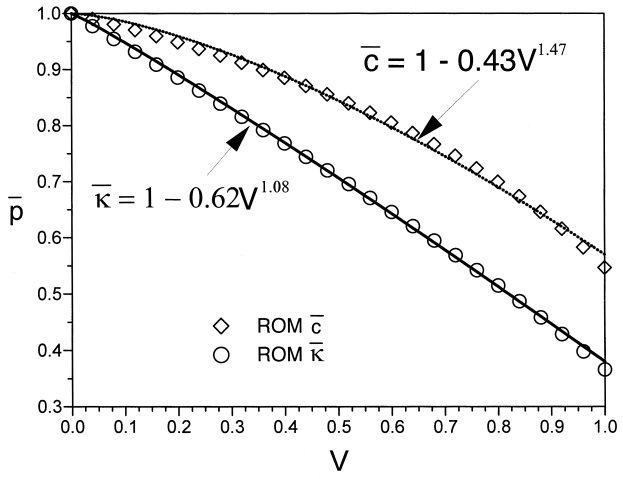

Fig. 10. Variation of normalized wave speeds and acoustic impedances with volume fraction of Aluminum.

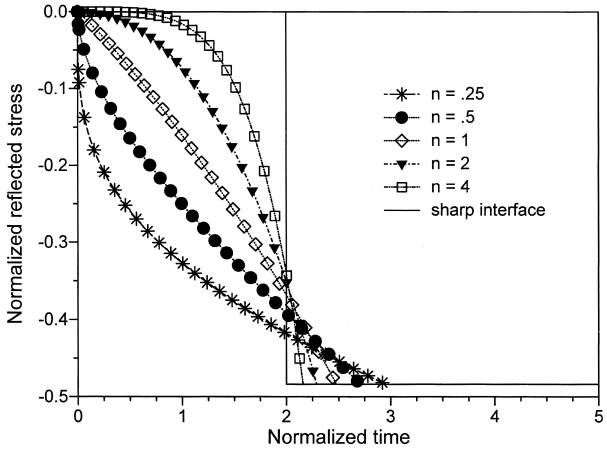

Fig. 11. Time-history of reflected stress pulse for Alumina–Aluminum FGM with various gradient architectures.

material properties increase.

6. Although time delay benefits are greatest with porous FGMs, termination of a porous FGM in a free surface at a porosity level less than 100% can result in larger peak reflected stresses that occur sooner than if a sharp interface were present.
7. For Alumina–Aluminum FGMs, the time delay benefits are so small for stresses approaching steady-state levels that only slight improvements in their energy absorbing capability may be expected.

From these conclusions, it appears that the optimal architecture for attenuating stress waves in FGMs will depend greatly upon the design stress for the reflected wave.

The proposed theoretical model can be experimentally verified by testing functionally graded specimens in a split Hopkinson pressure bar. The propagation of the stress wave through the specimen can be monitored by placing a strain gage on the first base material. It is important to remember that the signal from the strain gage will be a superposition of strains from the reflected and incident stress

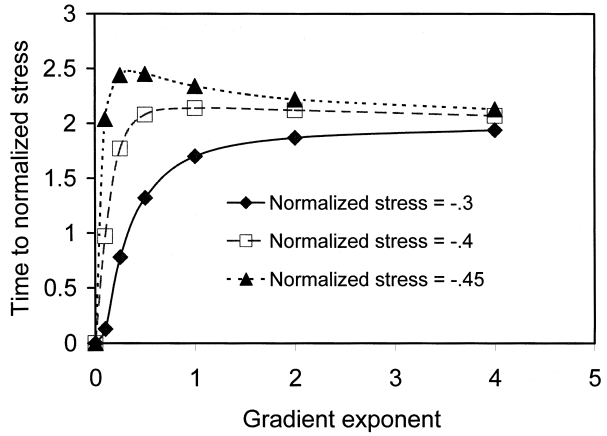

Fig. 12. Variation of time to normalized reflected stress with gradient exponent at various normalized stresses levels for Alumina–Aluminum FGM.

waves. Therefore, the strain gage should be placed a sufficient distance away from the graded interface to determine the contribution of the incident stress wave to the strain gage signal.

References

Dorf, R.C., 1986. Modern Control Systems, 4th ed. Addison-Wesley, Reading, MA.

Finot, M., Suresh, S., 1996. Small and large deformation of thick and thin-film multi-layers: effects of layer geometry, plasticity and compositional gradients. Journal of the Mechanics and Physics of Solids 44, 683–721.

Kuwahara, O., Wang, N., Ueha, S., 1992. Reconstruction of acoustic impedance distribution of functionally gradient materials by using reflection impulse response. Japanese Journal of Applied Physics 31 (1), 102–104.

Markworth, A.J., Ramesh, K.S., Parks Jr., W.P., 1995. Modeling studies applied to functionally graded materials. Journal of Materials Science 30, 2183–2193.

Meyers, M.A., 1994. Dynamic Behavior of Materials. John Wiley and Sons, New York, NY.

Mortenson, A., Suresh, S., 1995. Functionally graded metals and metal–ceramic composites. Part I: Processing. International Materials Reviews 40, 239–265.

Wilkins, M.L., Cline, C.F., Honodel, M.A., 1970. Fourth progress report of light armor program. Lawrence Livermore National Laboratory, UCRL-50694.

Williamson, R.L., Rabin, B.H., Drake, J.T., 1993. Finite element analysis of thermal residual stresses at graded ceramic–metal interfaces. Part I: Model description and geometrical effects. Journal of Applied Physics 74, 1310–1320.

Williamson, R.L., Rabin, B.H., 1996. The effect of interlayer properties on residual stresses in ceramic-metal joining. In: Proceedings of the American Ceramic Society 1996 Annual Meeting. Indianapolis, IN, April 14–17.